5th CIRP CSI 2020

Surface drag analysis after Ti-6Al-4V orthogonal cutting using grid distortion

A. Sela[a],*, G. Ortiz-de-Zarate[a], D. Soler[a], P. Aristimuño[a], D. Soriano[a], G. Germain[b], F. Ducobu[c], P.J. Arrazola[a]

[a]*Faculty of Engineering, Mondragon Unibertsitatea, 20500 Arrasate, Spain*
[b]*Arts et Métiers ParisTech, CER Angers - Laboratoire LAMPA - 2 Bd du Ronceray, 49035 Angers Cedex 1, France*
[c]*University of Mons (UMONS), Faculty of Engineering (FPMs), Machine Design and Production Engineering Lab 7000 Mons, Belgium*

* Corresponding author. Tel.: +34 943 712 185; fax: +34 943 000 500. *E-mail address:* asela@mondragon.edu

Abstract

Surface integrity directly affects the mechanical behavior of the workpiece, which is especially relevant on fatigue behavior. To characterize the quality of the machined surface, aspects such as material damage, roughness or residual stress are considered. Measurement of the material damage of the surface is characterized in some cases as surface drag, depth of the affected machining zone, a phenomenon which takes place due to plastic strain in the surface layer caused by machining stress which could have an influence on residual stress. Surface drag measurement done with optical microscopes has relevant uncertainty. In this paper, a methodology to measure the surface drag with lower uncertainty is proposed. The method consists of measuring the deformation of a grid as a result of the machining process. The grid was created with micromilling. The method was applied to analyze the effect of feed on the surface integrity after orthogonal cutting of Ti-6Al-4V. The depth of the affected layer was measured using a 3D optical measuring device (Alicona Infinite Focus IFG4) and compared with numerical simulations and a good agreement was achieved. In comparison with optical microscope results, it can be concluded that traditional method underestimates surface drag.

Keywords: Surface drag, surface integrity, orthogonal cutting, Ti-6Al-4V

1. Introduction

Titanium alloys, especially Ti-6Al-4V, are widely used in industry, being relevant in aeronautical applications, as well as automotive, chemical and medical ones [1]. Ti-6Al-4V is an $\alpha+\beta$ alloy which represents more than 50% of the production of the titanium alloys [2]. It is employed in industry because of the combination of good properties such as low density, high strength at elevated temperatures and corrosion resistance [3, 4].

However, in spite of these advantages, it is known as difficult-to-cut material due to its poor machinability because of its low thermal conductivity and high chemical activity, which is traduced in chip tool adhesion and segmentation, affecting the final surface of the workpiece [4–6].

There exist different ways to evaluate the final surface state, paying attention to material properties (hardness or residual stress), metallurgical and microstructural aspects (phase transformation, tearing or surface drag) or topological ones (roughness) [6–8]. This state is directly related to the final behavior of the workpiece and, especially, to its fatigue life [9]. Thus, special attention should be paid to finishing operations, as they define the surface state of the manufactured component.

Based on literature review, the surface integrity of aeronautical alloys such as Ti-6Al-4V has been widely studied, with special focus on aspects such as roughness, hardness or residual stress [6–8]. Other important aspects such as microstructural alterations or surface drag, depth of the affected machining zone, are usually not considered and few examples can be found in literature.

For instance, focused on titanium alloys, Che-Haron (2001) [10] and Grintin and Nouari (2009) [11] observed severe tearing and plastic deformation when turning Ti-6246, especially after prolonged machining and under dry conditions. In addition, when the tool failed, notable deformation of the microstructure was observed. Thus, phenomenon such as surface drag was observed to increase by using worn tools [10]. The same conclusions were obtained by Che-Haron and Jawaid (2005) for Ti-6Al-4V [12]. Puerta-Velásquez et al. (2010) studied the evolution of the microstructure of Ti-6Al-4V, for high cutting speeds (up to 600 m/min) [13]. They demonstrated that the thickness of the machining affected zone increased with cutting speed almost linearly. Joshi et al. (2015) [14] demonstrated that different environments (dry, cooling or LN2) for orthogonal cutting of Ti-6Al-4V have effect on machining affected zone. Li et al. (2017) analyzed microstructural surface evolution when high speed machining Ti-6Al-4V via FEM [15].

The majority of these studies were carried out at high speeds, not including broaching conditions on the analysis. However, broaching is a widely used operation in aerospace due to the good surface integrity condition obtained [1]. Thus, it is important to know the state of the machined surface at broaching conditions, usually characterized by low cutting speeds and feeds [16], [17]. Nevertheless, it has barely been studied in comparison to other machining operations such as turning or milling. In addition, Childs et al. (2018) [18] introduced a failure model, validated at low and high cutting speeds, to model the orthogonal cutting of Ti-6Al-4V. Some results of numerical surface drag were shown, but, as surface integrity was out of the scope of the paper, this issue was not deeply studied. Also an experimental and numerical comparison of surface drag for Ti-6Al-4V can be found in [1].

To the best of our knowledge, the study of surface drag is usually based on optical microstructure analysis and its effectiveness could depend on the microstructure obtained. Thus, this paper presents a methodology to measure the surface drag with an optical method, based on the distortion of a mechanical grid machined in the workpiece. In addition, these measurements were carried out at 7.5 m/min (broaching conditions) and were validated with FEM simulations and microstructure based measurements.

The paper is organized as follows. First, the experimental set-up is explained. Then, the numerical model is briefly shown. After that, numerical and experimental results are analyzed and discussed and some conclusions are finally drawn.

2. Experimental set-up

Orthogonal linear cutting tests were carried out on a vertical machine center Lagun CNC 8070. The workpiece material was Ti-6Al-4V. To prevent side flow problems it has been decided to machine two workpieces of 2 mm clamped together with the grid between two halves [19]. The workpiece was clamped to the machine table whereas the tool holder was set in the spindle. The set-up used is explained in the previous publication [20].

The insert used was an uncoated TPUN 160308, with a nominal edge radius of 25 μm (see Fig. 1), measured in an optical 3D measurement device (Alicona Infinite Focus IFG4), with an accuracy of 1 μm and a magnification of 10X.

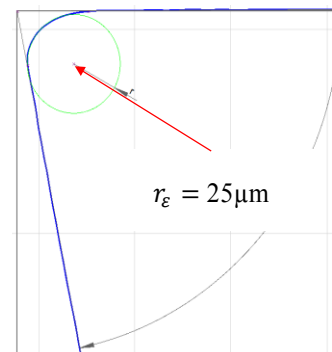
$$r_\varepsilon = 25\mu m$$

Fig. 1. Measurement of the edge radius

The effect of the feed (uncut chip thickness) on the surface integrity state was studied varying from 0.1 to 0.4 mm. The cutting speed was 7.5 m/min, typically used in broaching operations. The experimental plan, tool geometry and material are summarized in Table 1.

Table 1. Experimental plan

Tool	Ref.	TPUN 160308
	Rake angle, γ (°)	6
	Relief angle, α (°)	5
	Coating	Uncoated
	Edge radius, r_ε (μm)	25
Cutting conditions	Cutting speed, V_c (m/min)	7.5
	Feed, f (mm)	0.1, 0.2, 0.4
Lubrication	Type	Dry
Workpiece	Material	Ti-6Al-4V

To measure the surface drag, a mechanical grid was created using a KERN-EVO micromilling machine. The ball end mill used had 0.1 mm diameter, and a grid with a line separation of 0.04 mm was obtained. Fig. 2 shows the undeformed grid measured in a macroscopy device with a magnification of 6X. The grid state after the machining process was measured with the Alicona IFG4 with 50X magnification, to have enough resolution to carry out the measurement of the surface drag. The length of cut was 24 mm and notable repeatability was obtained along the whole length on surface drag measurement. For each cutting test new tool was used to avoid tool wear effects.

3. Numerical model

3.1. Material model

The measurements of the surface drag were compared with numerical results. In a previous publication, flow stress and damage law for Ti-6Al-4V were analyzed and determined [21].
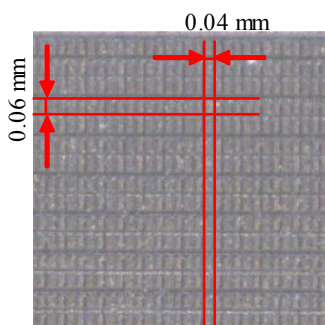
Fig. 3. Picture of the undeformed grid

Regarding flow stress model, Johnson and Cook model was proved to be accurate enough. Despite being a simple model compared to other flow stress laws, this model, with the parameters summarized in Table 2, takes into account the effects of isotropic hardening, strain rate hardening and thermal softening as showed in [21].

Table 2. Adjusted flow stress model parameters [21]

A (MPa)	B (MPa)	C	n	m	$\dot{\varepsilon}_0$
1130	530	0.0165	0.39	0.61	1

To represent the typical chip segmentation during machining of Ti-6Al-4V it is necessary to introduce a ductile failure model. The ductile failure model used was reported by Childs et al. (2018) [18] and it was demonstrated to be accurate at low and high cutting speeds, at least to predict cutting forces, chip morphology and temperature [18], [21]. At high cutting speeds, the failure is supposed to be due to thermal softening, which causes adiabatic shearing along the primary shear zone. However, at low cutting speeds as the one used in this research, the failure mechanism is governed by the lack of ductility, causing the segmentation of the chip. Thus, the failure model implemented had two different stages, decomposed into the initiation of the failure and the flow stress reduction due to this failure.

The Mohr-Coulomb failure law was chosen to represent the failure initiation [18], [21]. This model considers the accumulation of damage (D) along a streamline, where the damage is modelled as a function of the stress triaxiality (η) and failure coefficients ($\varepsilon_{f,0}$ and c). The effect of temperature was also taken into account, as it was observed to affect ductile failure.

The mechanical and thermal properties of the material and the tool were taken from literature [21].

3.2. Model description

The simulations were carried out in AdvantEdge 2D, which has a coupled thermo-elasto-plastic Lagrangian code with continuous remeshing and adaptive meshing [21]. The mesh was created with a minimum element size of 2 µm to ensure accurate results. The residual stress analysis was activated to achieve a fine mesh in the machined surface.

The material model previously explained was implemented in the software by user-defined subroutine developed in Fortran language.

To reduce the time to reach the steady state, the heat capacity of the tool was set to a value much lower than the physical one, as it was stated in [22].

Finally, to represent the tool-chip friction law, a sticking-sliding model was chosen and, due to the low cutting speeds, the friction coefficient was set to 1 according to [21].

The simulations were carried out following the same experimental plan as shown in Table 1.

4. Results and discussion

The main idea to measure the surface drag is to observe the affected zone with the Alicona IFG4 with a magnification of 50X. Due to the existence of a physical 3D grid in the workpiece it is possible to see whether it has been deformed by the machining process, and therefore to measure its depth. The red line in Fig. 3 shows Alicona's image of the workpiece after being machined with a feed of 0.2 mm. The red line marks the limit of the surface drag, placed at 47 µm of the machined surface.
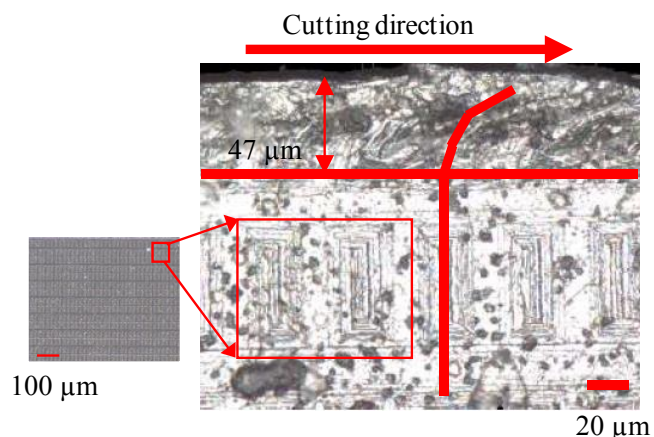

Fig. 2. Experimental surface state for $f = 0.2$ mm

These results can be compared with those obtained by numerical simulations (see Fig. 4). In this case, to obtain the surface drag, the strain was measured along different lines orthogonal to the machined surface.

The plastic strain of each line for each cutting condition was plotted against depth (Fig. 5). Due to the asymptotical behavior observed, it was decided that a strain of 0.02 is the threshold value to determine the limit of the drag zone [23]. Taking into account that the numerical measurements could be fitted with an exponential function, it has been stated that the surface drag in this case was 54 µm (7 µm of difference between numerical

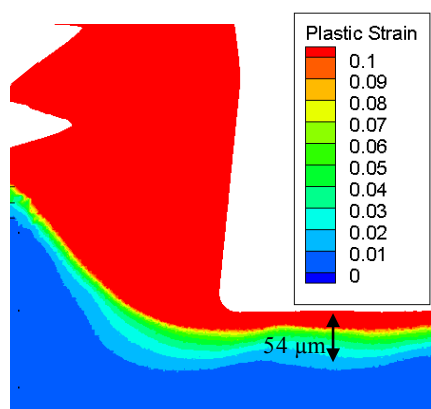and experimental values). The results for all cutting conditions are shown in Table 3.

Fig. 5. Numerical results for *f* = 0.2 mm

Fig. 5 shows that at low feeds (*f* = 0.1 and 0.2 mm), the obtained plastic strains were similar, being close to 7, at low depths (near the machined surface) and then it decreases
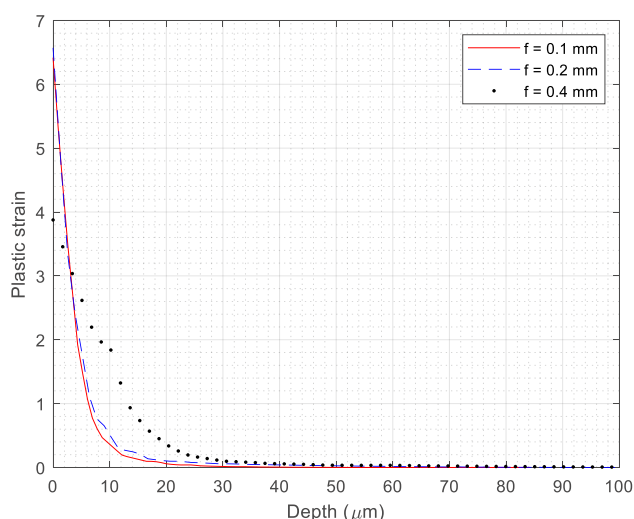

Fig. 6. Numerical plastic strain against depth of the machined surface at different feeds

drastically with depth. On the contrary, at the highest feed (0.4 mm), the strain at the machined surface was lower than 4 and the slope was less pronounced. This effect could be relevant on the quality of the machined surface.

In addition, experimental values were also compared with common measurements of surface drag based on microstructure alterations. For that, the sample was polished and chemically etched with Kroll. Then, the measurements were carried out in an optical microscope Leica with magnification of 50X (see Fig. 6). The measurements were carried out within the meshed workpiece, in the middle of this workpiece and located one millimeter away from the grid.

The measurement for each condition was repeated twice and the variations between each repetition were lower than 3 μm.
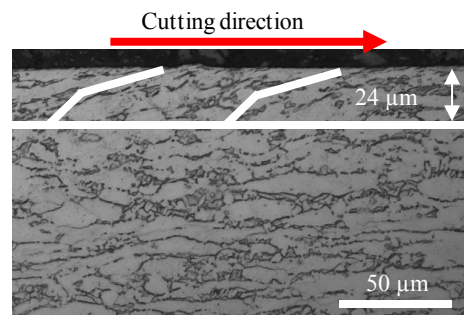

Fig. 4. Surface drag measurement for *f* = 0.2 mm based on microstructural alterations

In Table 3 all the results are summarized, including grid based, microstructural based (optical) and numerical values.

Table 3. Comparison of the results

f (mm)	Depth of the surface drag (μm)		
	Grid distortion	Optical	Numerical
0.1	20	15	28
0.2	47	25	54
0.4	90	37	75

The uncertainty of the measurements done with Alicona IFG4 device was of ± 5 μm based on grid dimensions and repeatability of the results along the length of cut. The results against feed are shown in Fig. 7. The error bar in the numerical results comes from the fact that strain was measured in several lines.
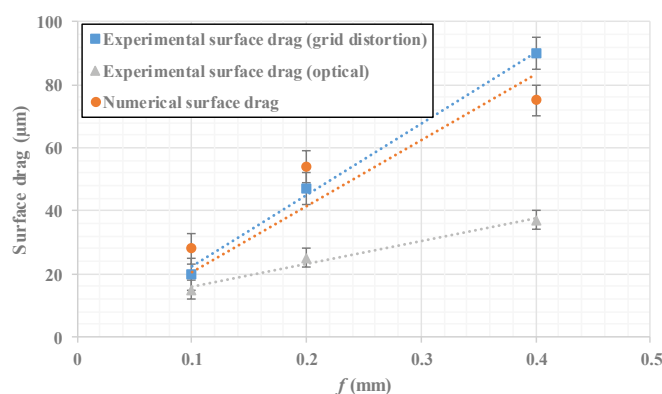

Fig. 7. Variation of surface drag against feed

In general, it was observed that the values reported by microstructure based measurements are notably lower than the ones measured with grid distortion and lower than the values predicted by the model, especially at high feeds.

Comparing both experimental techniques, at *f* = 0.1 mm, the difference was 5 μm, which is inside the range of uncertainty. However, these differences are more remarkable at higher feeds (being 22 μm for *f* = 0.2 mm and 53 μm for 0.4 mm). If these differences are plotted against feed, a behavior totally linear was observed (see Fig. 8). This suggests that the new method is more sensitive to material deformation than the microstructural change based method.

Between numerical and new method results, the differences were lower. It was around 8 μm for 0.1 and 0.2 mm and 15 μm for 0.4 mm, which could be considered a good agreement.

In addition, for the used cutting speed, new method results show a linear trend between surface drag and feed. A slope of 226 μm/mm (surface drag/feed) was obtained for the grid measurements.
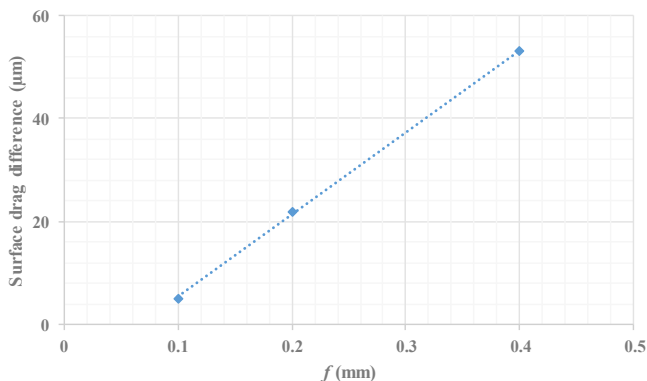

Fig. 8. Differences on surface drag measurements against feed between the two experimental techniques

5. Conclusions

A new technique to measure the surface drag was presented based on a mechanical grid. With this technique, it is not necessary to use the microstructure to obtain the surface drag, avoiding the intrinsic randomness associated with microstructural aspects.

Comparing both techniques, it was observed that microstructure is not able to reproduce the total amount of strain achieved as the machining affected zone is higher than the one measured using microstructural distortion.

As the accuracy of the technique presented depends on the dimension of the grid, the obtained value could be considered as a lower limit value of the surface drag and the machining affected zone could be even higher than the one measured with this method.

This technique was applied to characterize the surface drag of Ti-6Al-4V after orthogonal machining under cutting conditions close to broaching. The experimental results were compared with numerical ones achieving a good agreement, with errors about 8 μm at low feeds and 15 μm at the highest one.

The effect of the feed on surface drag was analyzed, and it was shown that there exists an increasing trend on surface drag when feed is increased. This trend is important, as the cutting speed tested is typical in the broaching process, which is commonly used as a finishing process. This confirms that to achieve good surface integrity low feeds should be used.

However, the plastic strain numerically observed was higher for low feeds, which can also be considered a bad point in terms of surface integrity.

References

[1] G. Ortiz-de-Zarate, A. Madariaga, A. Garay, L. Azpitarte, I. Sacristan, M. Cuesta, and P. Arrazola, "Experimental and FEM analysis of surface integrity when broaching Ti64," *Procedia Cirp*, vol. 71, pp. 466–471, 2018.

[2] P.-J. Arrazola, A. Garay, L.-M. Iriarte, M. Armendia, S. Marya, and F. Le Maıtre, "Machinability of titanium alloys (Ti6Al4V and Ti555. 3)," *Journal of materials processing technology*, vol. 209, no. 5, pp. 2223–2230, 2009.

[3] S. Cedergren, C. Frangoudis, A. Archenti, R. Pederson, and G. Sjöberg, "Influence of work material microstructure on vibrations when machining cast Ti-6Al-4V," *The International Journal of Advanced Manufacturing Technology*, vol. 84, no. 9–12, pp. 2277–2291, 2016.

[4] R. M'Saoubi, D. Axinte, S. L. Soo, C. Nobel, H. Attia, G. Kappmeyer, S. Engin, and W.-M. Sim, "High performance cutting of advanced aerospace alloys and composite materials," *CIRP Annals*, vol. 64, no. 2, pp. 557–580, 2015.

[5] C. Courbon, F. Pusavec, F. Dumont, J. Rech, and J. Kopac, "Tribological behaviour of Ti6Al4V and Inconel718 under dry and cryogenic conditions—Application to the context of machining with carbide tools," *Tribology International*, vol. 66, pp. 72–82, 2013.

[6] D. Ulutan and T. Ozel, "Machining induced surface integrity in titanium and nickel alloys: A review," *International Journal of Machine Tools and Manufacture*, vol. 51, no. 3, pp. 250–280, 2011.

[7] A. Thakur and S. Gangopadhyay, "State-of-the-art in surface integrity in machining of nickel-based super alloys," *International Journal of Machine Tools and Manufacture*, vol. 100, pp. 25–54, 2016.

[8] X. Liang, Z. Liu, and B. Wang, "State-of-the-art of surface integrity induced by tool wear effects in machining process of titanium and nickel alloys: A review," *Measurement*, vol. 132, pp. 150–181, 2019.

[9] A. Javidi, U. Rieger, and W. Eichlseder, "The effect of machining on the surface integrity and fatigue life," *International Journal of fatigue*, vol. 30, no. 10–11, pp. 2050–2055, 2008.

[10] C. Che-Haron, "Tool life and surface integrity in turning titanium alloy," *Journal of Materials Processing Technology*, vol. 118, no. 1–3, pp. 231–237, 2001.

[11] A. Ginting and M. Nouari, "Surface integrity of dry machined titanium alloys," *International Journal of Machine Tools and Manufacture*, vol. 49, no. 3–4, pp. 325–332, 2009.

[12] C. Che-Haron and A. Jawaid, "The effect of machining on surface integrity of titanium alloy Ti–6% Al–4% V," *Journal of materials processing technology*, vol. 166, no. 2, pp. 188–192, 2005.

[13] J. P. Velásquez, A. Tidu, B. Bolle, P. Chevrier, and J.-J. Fundenberger, "Sub-surface and surface analysis of high speed machined Ti–6Al–4V alloy," *Materials Science and Engineering: A*, vol. 527, no. 10–11, pp. 2572–2578, 2010.

[14] S. Joshi, A. Tewari, and S. S. Joshi, "Microstructural characterization of chip segmentation under different machining environments in orthogonal machining of Ti6Al4V," *Journal of Engineering Materials and Technology*, vol. 137, no. 1, p. 011005, 2015.

[15] G. Li, Y. Cai, and H. Qi, "Prediction of the critical cutting conditions of serrated chip in high speed machining based on linear stability analysis," *The International Journal of Advanced Manufacturing Technology*, vol. 94, no. 1–4, pp. 1119–1129, 2018.

[16] S. Mo, D. Axinte, T. Hyde, and N. Gindy, "An example of selection of the cutting conditions in broaching of heat-resistant alloys based on cutting forces, surface roughness and tool wear," *Journal of materials processing technology*, vol. 160, no. 3, pp. 382–389, 2005.

[17] A. Sela, G. Ortiz-de-Zarate, I. Arrieta, D. Soriano, P. Aristimuño, B. Medina-Clavijo, and P. Arrazola, "A mechanistic model to predict cutting force on orthogonal machining of Aluminum 7475-T7351 considering the edge radius," *Procedia CIRP*, vol. 82, pp. 32–36, 2019.

[18] T. H. Childs, P.-J. Arrazola, P. Aristimuno, A. Garay, and I. Sacristan, "Ti6Al4V metal cutting chip formation experiments and modelling over

a wide range of cutting speeds," *Journal of Materials Processing Technology*, vol. 255, pp. 898–913, 2018.

[19] H. Ghadbeigi, S. Bradbury, C. Pinna, and J. Yates, "Determination of micro-scale plastic strain caused by orthogonal cutting," *International Journal of Machine Tools and Manufacture*, vol. 48, no. 2, pp. 228–235, 2008.

[20] G. Ortiz-de-Zarate, A. Sela, M. Saez-de-Buruaga, M. Cuesta, A. Madariaga, A. Garay, and P. J. Arrazola, "Methodology to establish a hybrid model for prediction of cutting forces and chip thickness in orthogonal cutting condition close to broaching," *The International Journal of Advanced Manufacturing Technology*, vol. 101, no. 5–8, pp. 1357–1374, 2019.

[21] G. Ortiz-de-Zarate, A. Sela, F. Ducobu, M. Saez-de-Buruaga, D. Soler, T. Childs, and P. Arrazola, "Evaluation of different flow stress laws coupled with a physical based ductile failure criterion for the modelling of the chip formation process of Ti-6Al-4V under broaching conditions," *Procedia CIRP*, vol. 82, pp. 65–70, 2019.

[22] P.-J. Arrazola, P. Aristimuno, D. Soler, and T. Childs, "Metal cutting experiments and modelling for improved determination of chip/tool contact temperature by infrared thermography," *CIRP Annals*, vol. 64, no. 1, pp. 57–60, 2015.

[23] H. Ghadbeigi, C. Pinna, and S. Celotto, "Quantitative strain analysis of the large deformation at the scale of microstructure: comparison between digital image correlation and microgrid techniques," *Experimental mechanics*, vol. 52, no. 9, pp. 1483–1492, 2012.